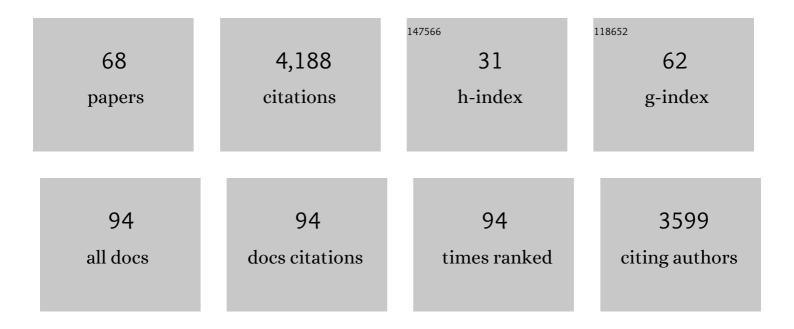
List of Publications by Year in descending order

Source: https://exaly.com/author-pdf/586538/publications.pdf Version: 2024-02-01



#	Article	IF	CITATIONS
1	Measurement of atmospheric nanoparticles: Bridging the gap between gas-phase molecules and larger particles. Journal of Environmental Sciences, 2023, 123, 183-202.	3.2	7
2	Influence of organic aerosol molecular composition on particle absorptive properties in autumn Beijing. Atmospheric Chemistry and Physics, 2022, 22, 1251-1269.	1.9	8
3	Modeling spatial variation of gaseous air pollutants and particulate matters in a Metropolitan area using mobile monitoring data. Environmental Research, 2022, 210, 112858.	3.7	9
4	Emissions of Ammonia and Other Nitrogen-Containing Volatile Organic Compounds from Motor Vehicles under Low-Speed Driving Conditions. Environmental Science & Technology, 2022, 56, 5440-5447.	4.6	19
5	Formation and growth of sub-3Ânm particles in megacities: impact of background aerosols. Faraday Discussions, 2021, 226, 348-363.	1.6	34
6	Impact of COVID-19 lockdown on ambient levels and sources of volatile organic compounds (VOCs) in Nanjing, China. Science of the Total Environment, 2021, 757, 143823.	3.9	29
7	Concentrations of total arsenic and arsenic species in PM2.5 in Nanjing, China: spatial variations and influences of local emission sources. Air Quality, Atmosphere and Health, 2021, 14, 271-281.	1.5	3
8	ls reducing new particle formation a plausible solution to mitigate particulate air pollution in Beijing and other Chinese megacities?. Faraday Discussions, 2021, 226, 334-347.	1.6	74
9	Sulfuric acid–amine nucleation in urban Beijing. Atmospheric Chemistry and Physics, 2021, 21, 2457-2468.	1.9	70
10	Radiatively driven NH3 release from agricultural field during wintertime slack season. Atmospheric Environment, 2021, 247, 118228.	1.9	2
11	The Synergistic Role of Sulfuric Acid, Bases, and Oxidized Organics Governing Newâ€₽article Formation in Beijing. Geophysical Research Letters, 2021, 48, e2020GL091944.	1.5	53
12	Uptake of Waterâ€soluble Gasâ€phase Oxidation Products Drives Organic Particulate Pollution in Beijing. Geophysical Research Letters, 2021, 48, e2020GL091351.	1.5	24
13	An indicator for sulfuric acid–amine nucleation in atmospheric environments. Aerosol Science and Technology, 2021, 55, 1059-1069.	1.5	19
14	Seasonality of nitrous acid near an industry zone in the Yangtze River Delta region of China: Formation mechanisms and contribution to the atmospheric oxidation capacity. Atmospheric Environment, 2021, 254, 118420.	1.9	4
15	Acid–Base Clusters during Atmospheric New Particle Formation in Urban Beijing. Environmental Science & Technology, 2021, 55, 10994-11005.	4.6	34
16	Mixing state and light absorption enhancement of black carbon aerosols in summertime Nanjing, China. Atmospheric Environment, 2020, 222, 117141.	1.9	29
17	Continuous and comprehensive atmospheric observations in Beijing: a station to understand the complex urban atmospheric environment. Big Earth Data, 2020, 4, 295-321.	2.0	54
18	Contribution of nitrous acid to the atmospheric oxidation capacity in an industrial zone in the Yangtze River Delta region of China. Atmospheric Chemistry and Physics, 2020, 20, 5457-5475.	1.9	21

#	Article	IF	CITATIONS
19	Carbenium ion-mediated oligomerization of methylglyoxal for secondary organic aerosol formation. Proceedings of the National Academy of Sciences of the United States of America, 2020, 117, 13294-13299.	3.3	28
20	Mechanism of the atmospheric chemical transformation of acetylacetone and its implications in night-time second organic aerosol formation. Science of the Total Environment, 2020, 720, 137610.	3.9	9
21	Responses of gaseous sulfuric acid and particulate sulfate to reduced SO2 concentration: A perspective from long-term measurements in Beijing. Science of the Total Environment, 2020, 721, 137700.	3.9	28
22	Seasonal Characteristics of New Particle Formation and Growth in Urban Beijing. Environmental Science & Technology, 2020, 54, 8547-8557.	4.6	78
23	Budget of nitrous acid and its impacts on atmospheric oxidative capacity at an urban site in the central Yangtze River Delta region of China. Atmospheric Environment, 2020, 238, 117725.	1.9	13
24	Effect of organic coatings derived from the OH-initiated oxidation of amines on soot morphology and cloud activation. Atmospheric Research, 2020, 239, 104905.	1.8	8
25	Significant restructuring and light absorption enhancement of black carbon particles by ammonium nitrate coating. Environmental Pollution, 2020, 262, 114172.	3.7	18
26	Observational Evidence for the Involvement of Dicarboxylic Acids in Particle Nucleation. Environmental Science and Technology Letters, 2020, 7, 388-394.	3.9	30
27	Evolution in physiochemical and cloud condensation nuclei activation properties of crop residue burning particles during photochemical aging. Journal of Environmental Sciences, 2019, 77, 43-53.	3.2	2
28	Light absorption properties and potential sources of particulate brown carbon in the Pearl River Delta region of China. Atmospheric Chemistry and Physics, 2019, 19, 11669-11685.	1.9	27
29	Characteristics of one-year observation of VOCs, NOx, and O3 at an urban site in Wuhan, China. Journal of Environmental Sciences, 2019, 79, 297-310.	3.2	68
30	On-line measurement of fluorescent aerosols near an industrial zone in the Yangtze River Delta region using a wideband integrated bioaerosol spectrometer. Science of the Total Environment, 2019, 656, 447-457.	3.9	12
31	The characteristics of abnormal wintertime pollution events in the Jing-Jin-Ji region and its relationships with meteorological factors. Science of the Total Environment, 2018, 626, 887-898.	3.9	71
32	Estimating the influence of transport on aerosol size distributions during new particle formation events. Atmospheric Chemistry and Physics, 2018, 18, 16587-16599.	1.9	17
33	OH-Initiated Oxidation of Acetylacetone: Implications for Ozone and Secondary Organic Aerosol Formation. Environmental Science & Technology, 2018, 52, 11169-11177.	4.6	43
34	Particle acidity and sulfate production during severe haze events in China cannot be reliably inferred by assuming a mixture of inorganic salts. Atmospheric Chemistry and Physics, 2018, 18, 10123-10132.	1.9	90
35	Atmospheric new particle formation from sulfuric acid and amines in a Chinese megacity. Science, 2018, 361, 278-281.	6.0	415
36	Data inversion methods to determine sub-3 nm aerosol size distributions using the particle size magnifier. Atmospheric Measurement Techniques, 2018, 11, 4477-4491.	1.2	20

#	Article	IF	CITATIONS
37	CCN activity of secondary aerosols from terpene ozonolysis under atmospheric relevant conditions. Journal of Geophysical Research D: Atmospheres, 2017, 122, 4654-4669.	1.2	12
38	Sizeâ€resolved measurements of mixing state and cloudâ€nucleating ability of aerosols in Nanjing, China. Journal of Geophysical Research D: Atmospheres, 2017, 122, 9430-9450.	1.2	22
39	Ageing and hygroscopicity variation of black carbon particles in Beijing measured by a quasi-atmospheric aerosol evolution study (QUALITY) chamber. Atmospheric Chemistry and Physics, 2017, 17, 10333-10348.	1.9	47
40	Aerosol surface area concentration: a governing factor in new particle formation in Beijing. Atmospheric Chemistry and Physics, 2017, 17, 12327-12340.	1.9	87
41	Detection of formaldehyde emissions from an industrial zone in the Yangtze River Delta region of China using a proton transfer reaction ion-drift chemical ionization mass spectrometer. Atmospheric Measurement Techniques, 2016, 9, 6101-6116.	1.2	46
42	An intensive study on aerosol optical properties and affecting factors in Nanjing, China. Journal of Environmental Sciences, 2016, 40, 35-43.	3.2	18
43	Markedly enhanced absorption and direct radiative forcing of black carbon under polluted urban environments. Proceedings of the National Academy of Sciences of the United States of America, 2016, 113, 4266-4271.	3.3	453
44	Source identification of trace elements in the atmosphere during the second Asian Youth Games in Nanjing, China: Influence of control measures on air quality. Atmospheric Pollution Research, 2016, 7, 547-556.	1.8	47
45	Reactions of Atmospheric Particulate Stabilized Criegee Intermediates Lead to High-Molecular-Weight Aerosol Components. Environmental Science & Technology, 2016, 50, 5702-5710.	4.6	54
46	Detection of atmospheric gaseous amines and amides by a high-resolution time-of-flight chemical ionization mass spectrometer with protonated ethanol reagent ions. Atmospheric Chemistry and Physics, 2016, 16, 14527-14543.	1.9	95
47	Nucleation and growth of sub-3 nm particles in the polluted urban atmosphere of a megacity in China. Atmospheric Chemistry and Physics, 2016, 16, 2641-2657.	1.9	55
48	Optical properties and chemical apportionment of summertime PM2.5 in the suburb of Nanjing. Journal of Atmospheric Chemistry, 2016, 73, 119-135.	1.4	7
49	Measurements of nitrous acid (HONO) in urban area of Shanghai, China. Environmental Science and Pollution Research, 2016, 23, 5818-5829.	2.7	25
50	Development of a new corona discharge based ion source for high resolution time-of-flight chemical ionization mass spectrometer to measure gaseous H 2 SO 4 and aerosol sulfate. Atmospheric Environment, 2015, 119, 167-173.	1.9	22
51	Measurement of atmospheric amines and ammonia using the high resolution time-of-flight chemical ionization mass spectrometry. Atmospheric Environment, 2015, 102, 249-259.	1.9	130
52	Measurements of submicron aerosols at the California–Mexico border during the Cal–Mex 2010 field campaign. Atmospheric Environment, 2014, 88, 308-319.	1.9	32
53	Measurements of nitrous acid (HONO) using ion drift-chemical ionization mass spectrometry during the 2009 SHARP field campaign. Atmospheric Environment, 2014, 94, 231-240.	1.9	35
54	Role of stabilized Criegee Intermediate in secondary organic aerosol formation from the ozonolysis of α-cedrene. Atmospheric Environment, 2014, 94, 448-457.	1.9	40

#	Article	IF	CITATIONS
55	Volatile organic compounds in Tijuana during the Cal-Mex 2010 campaign: Measurements and source apportionment. Atmospheric Environment, 2013, 70, 521-531.	1.9	25
56	Measurements of formaldehyde at the U.S.–Mexico border during the Cal-Mex 2010 air quality study. Atmospheric Environment, 2013, 70, 513-520.	1.9	22
57	Measurements of submicron aerosols in Houston, Texas during the 2009 SHARP field campaign. Journal of Geophysical Research D: Atmospheres, 2013, 118, 10,518.	1.2	56
58	Primary Sources and Secondary Formation of Organic Aerosols in Beijing, China. Environmental Science & Technology, 2012, 46, 9846-9853.	4.6	170
59	Laboratory Investigation on the Role of Organics in Atmospheric Nanoparticle Growth. Journal of Physical Chemistry A, 2011, 115, 8940-8947.	1.1	34
60	Submicron aerosol analysis and organic source apportionment in an urban atmosphere in Pearl River Delta of China using high-resolution aerosol mass spectrometry. Journal of Geophysical Research, 2011, 116, .	3.3	182
61	Atmospheric nanoparticles formed from heterogeneous reactions of organics. Nature Geoscience, 2010, 3, 238-242.	5.4	269
62	Overnight atmospheric transport and chemical processing of photochemically aged Houston urban and petrochemical industrial plume. Journal of Geophysical Research, 2010, 115, .	3.3	14
63	Atmospheric Pressure-Ion Drift Chemical Ionization Mass Spectrometry for Detection of Trace Gas Species. Analytical Chemistry, 2010, 82, 7302-7308.	3.2	39
64	Formation of nanoparticles of blue haze enhanced by anthropogenic pollution. Proceedings of the National Academy of Sciences of the United States of America, 2009, 106, 17650-17654.	3.3	244
65	Effects of Coating of Dicarboxylic Acids on the Massâ^'Mobility Relationship of Soot Particles. Environmental Science & Technology, 2009, 43, 2787-2792.	4.6	98
66	Enhanced Light Absorption and Scattering by Carbon Soot Aerosol Internally Mixed with Sulfuric Acid. Journal of Physical Chemistry A, 2009, 113, 1066-1074.	1.1	200
67	Effects of dicarboxylic acid coating on the optical properties of soot. Physical Chemistry Chemical Physics, 2009, 11, 7869.	1.3	99
68	Quantitative Analysis of Hydroperoxyl Radical Using Flow Injection Analysis with Chemiluminescence Detection. Analytical Chemistry, 2003, 75, 4696-4700.	3.2	29